

Raman spectroscopy of NiSe_2 and $\text{NiS}_{2-x}\text{Se}_x$ ($0 < x < 2$) thin films

This article has been downloaded from IOPscience. Please scroll down to see the full text article.

2000 J. Phys.: Condens. Matter 12 5317

(<http://iopscience.iop.org/0953-8984/12/24/320>)

View [the table of contents for this issue](#), or go to the [journal homepage](#) for more

Download details:

IP Address: 171.66.16.221

The article was downloaded on 16/05/2010 at 05:14

Please note that [terms and conditions apply](#).

Raman spectroscopy of NiSe₂ and NiS_{2-x}Se_x (0 < x < 2) thin films

C de las Heras† and F Agulló-Rueda‡

†Departamento Física de Materiales and Instituto Nicolás Cabrera, Facultad de Ciencias, Universidad Autónoma de Madrid, Cantoblanco, E-28049 Madrid, Spain

‡Materials Science Institute of Madrid, CSIC, Cantoblanco, E-28049 Madrid, Spain

Received 19 January 2000

Abstract. The Raman spectra of NiS_{2-x}Se_x (0 < x < 2) polycrystalline thin films have been measured for the first time in the whole x range and for NiSe₂. The NiSe₂ spectrum is qualitatively similar to the spectrum of NiS₂, but all frequencies are shifted to lower energies. The shift has been analysed in terms of the increment of the anion mass and the lattice expansion. Peaks in the Raman spectrum of the NiS_{2-x}Se_x alloy can be assigned to stretching and rotational modes of the S–S, Se–Se and S–Se pairs. The stretching vibration of the S–Se pairs shifts almost linearly from 400 cm⁻¹ for NiS₂ to 330 cm⁻¹ for NiSe₂. There is an accidental degeneracy between the S–S stretching and Se–Se libration frequencies. The relative Raman intensities fit well with a random occupation of the anion sites by S and Se atoms, and different scattering cross sections.

1. Introduction

The NiS_{2-x}Se_x system has been extensively investigated due to its rich phase diagram and interesting transport properties [1–5]. For x < 0.4 it is a semiconductor at all temperatures. For x > 0.6 it is metallic at all temperatures. For 0.4 < x < 0.6 it is a semiconductor at high temperatures, but under a critical temperature that depends on x, the material undergoes an insulator–metal transition. This change has been explained [5] by strong repulsive inter-ionic exchange interactions for the semiconducting phase and weaker repulsive interactions for the metallic phase. At the transition there is no change in the crystal structure [6–8].

Raman spectroscopy provides information on vibrational properties, crystal structure and bonding. It would be interesting to know if the changes in electronic properties mentioned above are accompanied by some anomalies in the lattice modes. Raman spectra have been reported for several pyrite-type compounds [9–13]. For the NiS_{2-x}Se_x alloy the Raman spectrum has been studied previously only in the x = 0–0.5 range [14–16]. No reports have been found for the end compound NiSe₂ nor for NiS_{2-x}Se_x in the x = 0.5–2 range.

2. Experimental

NiS_{2-x}Se_x thin films were prepared by sulphuration and selenation of Ni thin films thermally evaporated on a glass substrate in an Edward Auto 306 Coating System, as reported in [17]. During the deposition the thickness was controlled so that the Ni films obtained were about 0.15 μm thick.

Ni films were sulphurated/seleniated into closed ampoules where the correct amounts of sulphur and selenium to create a total pressure of 500 Torr, at the highest temperature, were

introduced. The ampoule was heated to a temperature of 723 K, which was maintained over 10 hours. During this process the thickness of the films increased to nearly $0.6 \mu\text{m}$. The amounts of sulphur and selenium introduced into the ampoule were calculated by considering both of them to be diatomic gases at the temperature of 723 K, and using the perfect gas equation. The selenium partial pressure was calculated using Dalton's law. Under the optical microscope, the surface of the samples presented some texture, as shown in figure 1.

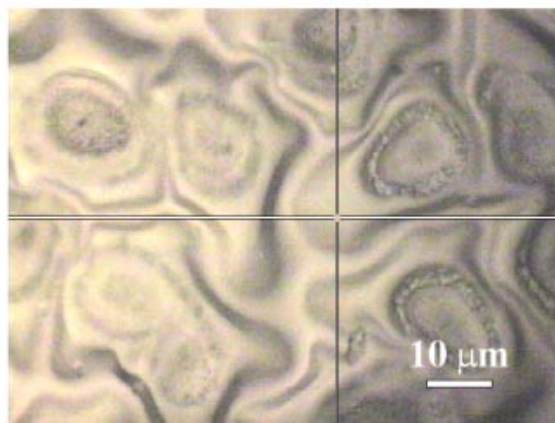


Figure 1. Micrograph of the surface for a $\text{NiS}_{2-x}\text{Se}_x$ sample with $x = 0.75$.

The structure of the samples and the selenium content in each one was detected by x-ray diffraction, recorded [18] by a Siemens D5000 diffractometer in the usual θ - 2θ couple mode with monochromatized $\text{Cu K}\alpha$ ($\lambda = 1.5418 \text{ \AA}$) radiation, working at 40 kV and 30 mA. A secondary graphite monochromator served to suppress the $\text{Cu K}\beta$ radiation. All diagrams were collected from 20° (2θ) to 120° (2θ) in the step scanning mode, with a 0.02° (2θ) step scanning and 2 s counting time. Divergence slits located in the incident beam were selected to ensure complete illumination of the surface at 15° (2θ). All x-ray experiments were carried out at 293 K. The least square structure refinements were undertaken with the full profile, Rietveld type program DBWS-9006PC, prepared by Sakthivel and Young. Grain size was calculated from the refined 2θ positions and the full width at half maximum of the reflections and values in the interval 500–1000 \AA were obtained.

Room temperature Raman spectra were taken with a Renishaw Ramascope spectrometer, equipped with an Ar^+ ion laser as a light source operating at a wavelength of 514.5 nm and focused on the sample through an optical microscope. The power density on the surface was of the order of 100 kW cm^{-2} . Light backscattered by the sample was collected with the same microscope and analysed with a single-grating spectrograph and a CCD detector. Reflected and elastically scattered light was blocked with two holographic filters, which also removed most of the Raman spectrum below 100 cm^{-1} . Unless otherwise indicated, no polarization analyser was used to select the scattered light. The Raman spectra did not change significantly between different points of the sample surface, indicating that the texture of the samples does not reflect chemical changes.

3. Results

3.1. Structure

NiS_{2-x}Se_x samples have been obtained for x in the interval 0–2 and characterized as pyrite type structures, belonging to the group $T_h^6(Pa3)$, as shown from an x-ray powder diffraction pattern. Samples were polycrystalline thin films with a grain size in the 500–1000 [Å] range. Lattice parameter a and selenium content x_{Se} have been obtained from the x-ray refining, and it has been seen that these follow a Vegar law, $a = (5.688 + 0.127x_{Se}) \text{ \AA}$. From the value of a , the anion–anion ($X-X$) and anion–cation (Ni– X) distances can be derived:

$$d(X - X)[\text{Å}] = 2.091 + 0.149x_{Se}$$

and

$$d(Ni - X)[\text{Å}] = 2.402 + 0.042x_{Se}.$$

The cubic unit cell contains four formula units. The metal atoms and the centres of the anion pairs occupy the sites of fcc lattices, so that in this respect the structure may be referred to as NaCl-like by replacing the Na atoms by Ni and Cl atoms by anion pairs (sulphur/selenium). The axis of the pairs is aligned along the four equivalent (111) directions.

3.2. Vibrational properties

The pyrite structure has five active Raman modes, which can be classified into the following symmetry species

$$\Gamma_{\text{vib}} = A_g + E_g + 3T_g.$$

Because Ni atoms are at the centre of inversion, Raman modes involve only movements of the X ions. Therefore, the Raman spectrum is very sensitive to the substitution of sulphur atoms by selenium. The A_g and $T_g(1)$ modes correspond, respectively, to in-phase and out-of-phase stretching vibrations of the $X-X$ pairs. $T_g(2)$, $T_g(3)$, and E_g modes correspond to librations of the $X-X$ pairs [11].

Figure 2 shows the Raman spectra measured at room temperature for the NiS_{2-x}Se_x alloy with different x values. The spectrum for the end compound NiS₂ is very similar to the spectrum reported by Suzuki *et al* [14]. The frequencies of the peaks and their assignments are listed in table 1. The two weak peaks at low energy correspond to the S–S pair librational modes, with symmetries T_g and E_g . The two strong peaks at higher energy correspond to stretching modes of the S–S pair, with symmetries A_g and T_g . The other T_g mode predicted by group theory corresponds to a S–S libration [11] and should appear close to the other librational modes. Therefore the Raman peak observed by Suzuki *et al* [14] at 596 cm⁻¹, which they assigned to a T_g species, could have a different origin.

On the other end of the alloy, the Raman spectrum of NiSe₂ corresponds to $x = 2$ in figure 2. As far as we know, this spectrum has not been reported before in the literature.

Table 1. Raman frequencies of the NiS_{2-x}Se_x end compounds in cm⁻¹.

Symmetry	NiS ₂	NiSe ₂
T_g	274.0	151.9
E_g	284.8	170.2
A_g	479.7	214.0
T_g	489.8	243.3

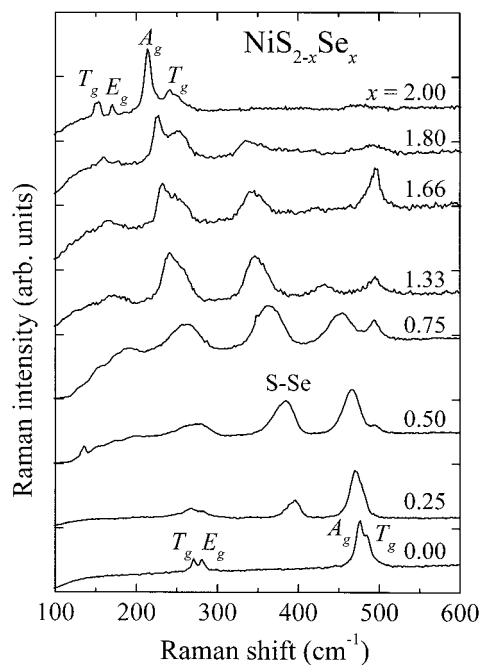


Figure 2. Raman spectra of the $\text{NiS}_{2-x}\text{Se}_x$ for indicated values of x .

Table 2. Dynamical parameters for the S–S, Se–Se, and S–Se pairs. Anion–anion distance, d , reduced mass, μ and moment of inertia, I .

	S–S (NiS_2)	Se–Se (NiSe_2)	S–Se
$d(\text{X–X})$ (\AA)	2.080	2.488	
μ (amu)	16	39.5	22.8
I (amu \AA^2)	69.2	244.5	

The measured spectrum is qualitatively similar to the spectrum of NiS_2 , but all frequencies are shifted to lower energy, due to the replacement of S atoms by Se. Table 1 shows the assignment of the Raman modes based on the assignment for NiS_2 and the anion mass ratio. The downward shift arises both from the mass increment and from the lattice expansion. The former increases the reduced mass, μ , of the stretching modes and the moment of inertia, I , of the librational modes (see table 2). The latter changes the force constants. With the dynamical parameters of the X–X pairs we can estimate the stretching and librational frequencies of the pair in NiSe_2 from the values observed in NiS_2 to help in the assignment for the latter. We will consider the average frequencies, weighted for degeneracy, of the stretching and the librational doublets, respectively. Assuming that stretching force constants vary as d^{-3} , the average stretching frequency of NiSe_2 would be $\nu = 483(\mu_{\text{S–S}}/\mu_{\text{Se–Se}})^{1/2}(d_{\text{Se–Se}}/d_{\text{S–S}})^{3/2} = 236 \text{ cm}^{-1}$, which is the observed value. For the librational modes, the effect of the lattice expansion is difficult to quantify. The change in the moment of inertia alone would give an average frequency of $\nu = 275\sqrt{I_{\text{S–S}}/I_{\text{Se–Se}}} = 146 \text{ cm}^{-1}$, which is smaller than the observed value of 159 cm^{-1} . In this case the lattice expansion produces a strengthening of the force constant. The Davydov splitting of the doublets also changes with the replacement of S atoms by Se; it increases from about 10 to 30 cm^{-1} for the stretching modes and from 10 to 20 cm^{-1} for the librational modes,

respectively. Therefore, although the lattice expands, the vibrational coupling between X–X pairs increases.

The Raman spectrum of the NiS_{2-x}Se_x alloy shows a complex behaviour with several modes, which can be assigned to the vibrations of S–S, Se–Se and S–Se pairs. As x increases from 0 the stretching mode doublet of the NiS₂ evolves into a broad band involving stretching vibrations of the S–S pairs [15] of the alloy. As expected, its intensity decreases, following the population of S–S units, and disappears for NiSe₂. Similarly, at the other end of the alloy, when x decreases from 2, the stretching doublet of NiSe₂ evolves into a broad band involving stretching vibrations of the Se–Se pairs. Its intensity reflects the population of Se–Se pairs and thus disappears for NiS₂. The frequency of these modes depends on the reduced masses and on the force constants. The former does not change with x , because the atoms remain the same for each pair. The latter changes mostly due to the lattice expansion, causing a decrease of the frequencies.

In the frequency region between the stretching modes of NiS₂ and NiSe₂ there is a peak that shifts almost linearly from 400 cm⁻¹ for NiS₂ to 330 cm⁻¹ for NiSe₂, which corresponds to the stretching vibration of mixed S–Se pairs [15]. This assignment is supported by the fact that its intensity vanishes for the two end compounds and reaches a maximum for $x \sim 1$. The presence of this peak shows that S–Se pairs are formed [15], in contrast with other systems with the pyrite structure, such as RuS_xSe_{2-x}, where S and Se do not bond together [13]. The frequency of this mode changes due to the change in the force constant, which accounts for the lattice expansion. In the range $0 < x < 0.55$ Lemos *et al* [15] found that the force constant was very similar to the force constant for the S–S A_g . In effect, considering only the difference in reduced masses, from the stretching frequency of the S–S pair at $x = 0$, one estimates a stretching frequency of 399 cm⁻¹ for the S–Se pair, which is close to the observed value. Accordingly, on the other end ($x = 2$), one could expect that the force constant of the S–Se stretching mode would be very similar to that of the Se–Se pair. However, under this assumption one estimates from the stretching frequency of the Se–Se pair a frequency of 282 cm⁻¹ for the S–Se pair, which is much lower than the observed value. It becomes apparent that the force constant of the S–Se pair is similar to the value for the S–S pair but is larger than the value for the Se–Se pair for the same lattice parameter.

Due to a fortuitous coincidence the Se–Se stretching frequencies of NiSe₂ are very close to the S–S librational frequencies of NiS₂. In the spectra (see figure 2) the librational peaks of NiS₂ seem to evolve continuously into the stretching peaks of NiSe₂, as can be seen in figure 3. Full lattice dynamics calculations could show whether this behaviour is due to an existence in the alloy of mixed modes involving Se–Se stretchings and S–S librations. The Se–Se librations of the NiSe₂ shift to higher energies in the NiS_{2-x}Se_x alloy as x decreases, and for $x = 0.55$ they move close to 200 cm⁻¹. From this it is clear that the unidentified mode observed by Lemos [15] at 200 cm⁻¹ for $x = 0.55$ corresponds to Se–Se librations.

Finally, there is a peak near to 500 cm⁻¹, whose frequency does not change with x and whose intensity is zero for the end compounds and reaches a maximum for around $x = 1.7$. Since its frequency is very close to the stretching frequency of S–S pairs and it does not shift, one could speculate with the presence of NiS₂ precipitates within the NiS_{2-x}Se_x alloy or with disorder-activated peaks. However, at present we do not know the physical origin of this peak.

A good test to prove the assignments of the Raman peaks to pair vibrations is given by their intensities versus x . We have already pointed out that they should be proportional to the population of the corresponding pair. Assuming that there is a random substitution of S by Se ions, the intensity of a mode involving an X–Y pair is proportional to the product of the concentration ions X and Y, multiplied by a factor that accounts for the different scattering efficiencies. Since it is difficult to get absolute intensities from the experiments or to compare

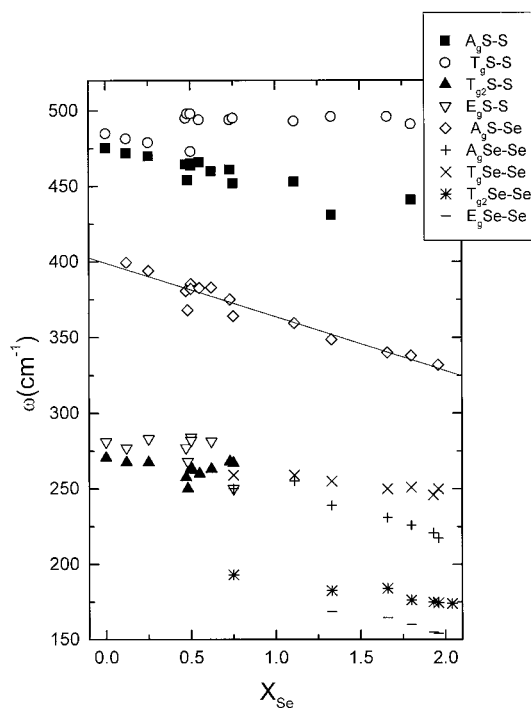


Figure 3. Frequency of the vibrational modes versus x obtained from the Raman spectra. Continuous line is the least square fit of the S–Se frequencies: $\omega(\text{S–Se}) = 400 - 35.35x_{\text{Se}}$.

Table 3. The Raman intensity for the stretching modes of X – Y pairs versus x , assuming a random occupation of pair sites by S and Se anions. Relative intensities are normalized to the S–Se mode.

X – Y pairs	Intensity	Relative intensity
S–S	$C_{\text{S–S}}(2-x)^2$	$(C_{\text{S–S}}/C_{\text{S–Se}})(2-x)/x$
S–Se	$C_{\text{S–Se}}(2-x)x$	1
Se–Se	$C_{\text{Se–Se}}x^2$	$(C_{\text{Se–Se}}/C_{\text{S–Se}})x/(2-x)$

data from different spectra we have compared the intensities of the S–S and Se–Se stretching modes relative to the intensity for the S–Se modes, which cover a wider range of x . The expected dependence with x is given in table 3 and the comparison with the measured values is shown in figure 4. Experimental data follow the expected trend very well. The constants C_1 and C_2 obtained from the fitting of the curves are 0.555 and 0.357, respectively, showing that the S–S stretching mode has a Raman intensity larger than the Se–Se stretching mode.

4. Conclusions

The Raman spectra of polycrystalline $\text{NiS}_{2-x}\text{Se}_x$ thin films have been obtained for the whole range of x . The assignment of the modes has been made according to previous work in the range $0.0 < x < 0.5$. The observed modes have been identified as stretching and librations of the S–S, Se–Se and S–Se pairs. A new mode of the alloy has been identified as a Se–Se libration. The relative frequencies of the modes and their variation with x has been analysed

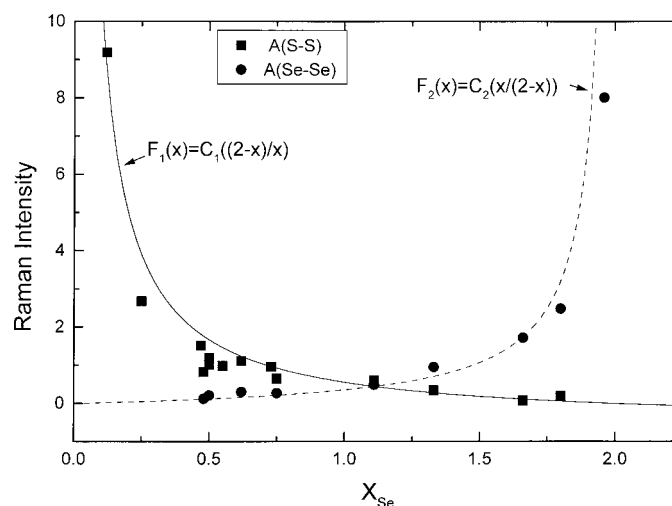


Figure 4. Raman intensity versus x for the S–S and Se–Se stretching modes normalized by the S–Se stretching mode intensity (points). The curves correspond to $C_1[(2-x)/x]$ and $C_2[x/(2-x)]$ with $C_1 = 0.555$ and $C_2 = 0.357$, respectively (see table 3).

in terms of the reduced masses or moment of inertia and the lattice expansion when S atoms are substituted by Se. An accidental degeneracy between the S–S librational and the Se–Se stretching modes has been found. The relative Raman intensity of the modes versus x is explained to a good approximation by a random occupation of pair sites by S and Se atoms.

Acknowledgments

We acknowledge financial support from the Spanish CICYT (projects MAT96-0395-CP, MAT97-0725, and PB97-0033).

References

- [1] Wilson J A and Pitt G D 1971 *Phil. Mag.* **23** 1297
- [2] Honig J M and Spalek 1998 *Chem. Mater.* **10** 2910
- [3] Bouchard R J, Gillson J L and Jarrett H S 1973 *Mater. Res. Bull.* **8** 489
- [4] Jarret M S, Bouchard R J, Gillson J L, Jones G A, Marcus S M and Weiher J F 1973 *Mater. Res. Bull.* **8** 877
- [5] Kwizera P K, Dresselhaus M S and Adler D 1980 *Phys. Rev. B* **21** 2328
- [6] Endo S, Mitsui T and Miyada 1973 *Phys. Lett. A* **46** 29
- [7] Yao X, Honig J M, Hogan T, Kannewurf C and Spelek J 1996 *Phys. Rev. B* **54** 17469
- [8] Husmann A, Jin D S, Zastavker Y V, Rosenbaum T F, Yao X and Honig J M 1996 *Science* **274** 1874
- [9] Vogt H, Chattopadhyey T and Stolz H J 1983 *J. Phys. Chem. Solid* **44** 869
- [10] Müller B and Lutz H D 1991 *Phys. Chem. Minerals* **17** 716
- [11] Lutz H D, Himmrich J, Müller B and Schneider G 1992 *J. Phys. Chem. Solids* **53** 815
- [12] Taguchi I, Vaterlaus H P, Bichsel R, Levy F, Berger H and Yumoto M 1987 *J. Phys. C.: Solid State Phys.* **20** 4241
- [13] Stingl Th, Müller B, Lutz H D 1992 *J. Alloys Compounds* **184** 275
- [14] Suzuki T, Uchinocura K, Sakine T and Matsura E 1977 *Solid State Commun.* **23** 847
- [15] Lemos V, Gualteco G M, Salzberg J B and Cerdeira F 1980 *Phys. Status Solidi b* **100** 755
- [16] Miyadai T, Tazuke Y, Kinouchi S, Nishioke T, Sudo S, Miyako Y, Watanabe K and Inoue K 1988 *J. Physique* **49** C8 187

- [17] Otero R, Martín de Vidales J L and de las Heras C 1998 *J. Phys.: Condens. Matter* **10** 6919
- [18] de las Heras C, Martín de Vidales J I, Ferrer J I and Sánchez C 1996 *J. Mater. Res.* **11** 211
- [19] Anastassakis E and Perry C H 1976 *J. Chem. Phys.* **64** 3604
- [20] Sourisseau C, Cavegnat R and Fouassier M 1991 *J. Phys. Chem. Solid* **52** 537